Articles

QSAR Studies on 6-Nitroquipazine Analogues as Serotonin Transporter

In Young Lee, Kyung A Lee, Bon-Su Lee, Dae Yoon Chi, and Chan Kyung Kim*

*Department of Chemistry, Inha University, Incheon 402-751, Korea. *E-mail: kckyung@inha.ac.kr*
Received June 13, 2006

3D-QSAR model that correlates the biological activities with the chemical structures of quipazine derivatives acting on the serotonine transporter (SERT) was developed by comparative molecular field analysis (CoMFA). Total 8 models were constructed and a more accurate model, using close 1 Å grid spacing and StDev*Coefficients weight value gave better results. The contour maps with the best model, the resulting cross-validated correlation (q^2 = 0.744), and non-cross-validated correlation (r^2 = 0.966) indicate the steric and electrostatic environment of inhibitors in the SERT binding pocket. This study can be used as a putative picture of the pharmacophore in the design of novel and potent inhibitors.

Key Words : CoMFA, Serotonine transporter, 6-Nitroquipazine analogues

Introduction

In recent years, much interest based on the implication of the serotoninergic system, which is related to several neuropsychiatric diseases including depression, anxiety, and schizophrenia in human brain has been shown.[1,2] The serotonin transporter (SERT) plays a key role in the regulation of synaptic serotonin(5-hydroxytryptamine, 5-HT) levels. The human SERT (hSERT) is a 630 amino acid protein with 12 putative membrane spanning helices and intracellular amino and carboxy termini,[3-6] but unfortunately its 3D structure is not known yet. So, most studies have been only concentrated on the ligands acting on the SERT. 5-HT reuptake sites in the mammalian brain have been studied extensively with radiotracers such as [^{3}H]imipramine, [^{3}H]paroxetine, and [^{3}H]citalopram. 6-Nitroquipazine (6-NQ) has been known as one of the most potent and selective antagonists for serotonin transporter *in vitro*[7,8] and *in vivo*,[9,10] showing higher potency (K_i = 0.17 nM) than paroxetine (K_i = 0.58 nM) or citalopram (K_i = 1.50 nM) for 5-HT reuptake site.

To analyze quantitative structure and activity relationship (QSAR), we have performed Comparative Molecular Field Analysis (CoMFA)[11] using various quipazine analogues, for which their biological activities (pK_i) were known.

Methods

Data sets and biological activity. QSAR analysis using CoMFA with 70 various quipazine analogues which were reported by D. Y. Chi *et al.* was accomplished.[12-14] Table 1 represents the structure and their biological activities (serotonin transporter affinity expressed as pK_i values, nM) of compounds employed in this study.

Computational details. All computational studies were performed using the molecular modeling program SYBYL 6.8.[15] running on a Silicon Graphics octane workstation. Structures were energy-minimized using the SYBYL energy minimizer (Tripos Force Field) with a 0.005 kcal/mol energy gradient convergence criterion and Gasteiger-Hückel charge. Low energy conformation was searched with systematic search, which is performed by rotating the torsional angle of a single bond by 30° interval. One of the conformers of 6-nitroquipazine compound (C1) having the lowest energy was then used as a template for alignment.

The CoMFA training set was composed of 70 compounds which were optimized and aligned based on the non-hydrogen atoms of the quipazine moiety of the template structure common to all compounds (Figure 1).

Steric and electrostatic fields were calculated at each three dimensional lattice of a regularly spaced grid of 2 Å and denser 1 Å. From these intervals, total 8 CoMFA sets were composed after applying region focusing method.

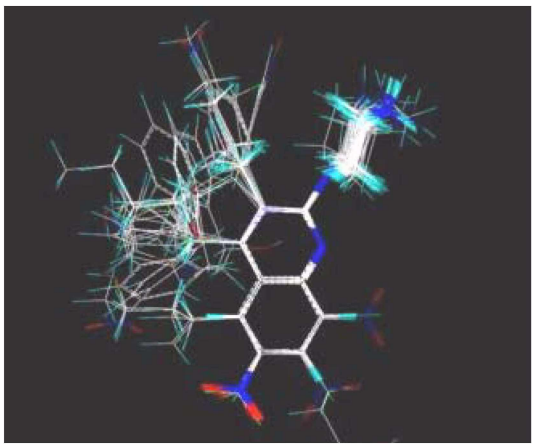

Figure 1. Stereoview of the 70 compounds aligned.

Table 1. Training set molecules and their biological activities used for 3D-QSAR analyses

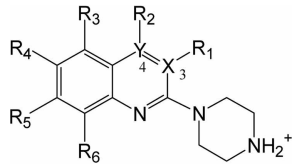

No	X	Y	R_1	R_2	R_3	R_4	R_5	R_6	K_i (nM)	pK_i
C1	C	C	H	H	H	NO_2	H	H	0.17 ± 0.03	9.77
C2	C	C	CH_3	H	H	NO_2	H	H	8.45 ± 0.62	8.07
C3	C	C	C_2H_5	H	H	NO_2	H	H	0.36 ± 0.02	9.44
C4	C	C	C_3H_7	H	H	NO_2	H	H	0.26 ± 0.01	9.58
C5	C	C	C_3H_6F	H	H	NO_2	H	H	0.32 ± 0.01	9.49
C6	C	C	C_5H_{11}	H	H	NO_2	H	H	1.69 ± 0.67	8.77
C7	C	C	Br	H	H	NO_2	H	H	12.62 ± 1.44	7.90
C8	C	C	H	CH_3	H	NO_2	H	H	0.24 ± 0.03	9.62
C9	C	C	H	C_2H_5	H	NO_2	H	H	9.79	8.01
C10	C	C	H	$CH=CH_2$	H	NO_2	H	H	1.42	8.85
C11	C	C	H	C_2H_4OH	H	NO_2	H	H	40.21	7.40
C12	C	C	H	C_3H_6OH	H	NO_2	H	H	79.09	7.10
C13	C	C	H	C_3H_6F	H	NO_2	H	H	12.14	7.92
C14	C	C	H	Cl	H	NO_2	H	H	0.017 ± 0.01	10.77
C15	C	C	H	I	H	NO_2	H	H	1.94	8.71
C16	C	C	H	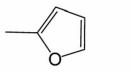	H	NO_2	H	H	5.23 ± 0.78	8.28
C17	C	C	H	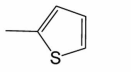	H	NO_2	H	H	67.24	7.17
C18	C	C	H	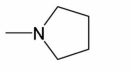	H	NO_2	H	H	61.12	7.21
C19	C	C	H	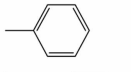	H	NO_2	H	H	60.03 ± 25.37	7.22
C20	C	C	H	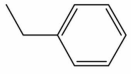	H	NO_2	H	H	126.86	6.90
C21	C	C	H	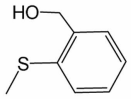	H	NO_2	H	H	144	6.84
C22	C	C	H	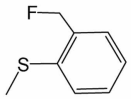	H	NO_2	H	H	227	6.64
C23	C	C	H	H	C_2H_5	NO_2	H	H	1.30 ± 0.26	8.89
C24	C	C	H	H	$CH=CH_2$	NO_2	H	H	0.05	10.30
C25	C	C	H	H	C_3H_6OH	NO_2	H	H	23.92 + 0.30	7.62
C26	C	C	H	H	C_3H_6F	NO_2	H	H	3.69 ± 0.26	8.43
C27	C	C	H	H	C_4H_9	NO_2	H	H	20.24	7.69
C28	C	C	H	H	$C_2H_4N(Me)_2$	NO_2	H	H	73.85	7.13
C29	C	C	H	H	H	CF_3	H	H	3.27 ± 0.21	8.48
C31	C	C	H	H	H	Br	H	H	0.91 ± 0.07	9.04
C30	C	C	H	H	H	Cl	H	H	1.68 + 0.13	8.77
C32	C	C	H	H	H	NO_2	Br	H	5.73 ± 1.65	8.24
C33	C	C	H	H	H	NO_2	C_3H_6OH	H	113.90	6.94
C34	C	C	H	H	H	NO_2	H	NO_2	312.85 + 2.85	6.50
C35	C	C	CH_3	Cl	H	NO_2	H	H	2.70 ± 0.32	8.57
C36	C	C	C_2H_5	Cl	H	NO_2	H	H	5.56 ± 0.54	8.25
C37	C	C	C_3H_7	Cl	H	NO_2	H	H	3.97 + 0.53	8.40

Table 1. Continued

No	X	Y	R_1	R_2	R_3	R_4	R_5	R_6	K_i (nM)	pK_i
C38	C	C	iso-C_3H_7	Cl	H	NO_2	H	H	321.24 + 5.03	6.49
C39	C	C		Cl	H	NO_2	H	H	1386.33	5.86
C40	C	C		Cl	H	NO_2	H	H	685.17 = 50.94	6.16
C41	C	C		Cl	H	NO_2	H	H	330.86 = 33.16	6.48
C42	C	C	CH_3	Br	H	NO_2	H	H	3.21 ± 0.03	8.49
C43	C	C	C_2H_5	Br	H	NO_2	H	H	5.85 ± 0.32	8.23
C44	C	C	C_3H_7	Br	H	NO_2	H	H	2.23 ± 0.46	8.65
C45	C	C	iso-C_3H_7	Br	H	NO_2	H	H	485.73 = 34.07	6.31
C46	C	C	C_4H_9	Br	H	NO_2	H	H	35.72 ± 1.87	7.45
C47	C	C			H	NO_2	H	H	50.52 ± 13.03	7.30
C48	C	C			H	NO_2	H	H	461.06 = 20.35	6.34
C49	C	C			H	NO_2	H	H	304.98 ± 2.83	6.52
C50	C	C			H	NO_2	H	H	226.90	6.64
C51	C	C	H	H	Br	NO_2	H	Br	103.32 ± 8.50	6.99
C52	C	N			H	NO_2	H	H	900.50 ± 74.10	6.05
C53	C	N	CH_3	H	H	H	NO_2	H	3470.5 ± 55.50	5.46
C54	N	C	–	OCH_3	H	NO_2	H	H	101.06 ± 16.19	6.99
C55	N	C	–	OC_2H_5	H	NO_2	H	H	288.17 = 29.69	6.54
C56	N	C	–	OC_3H_7	H	NO_2	H	H	288.17 = 29.69	6.54
C57	N	C	–	$OCH(Me)_2$	H	NO_2	H	H	217.05	6.66
C58	N	C	–		H	NO_2	H	H	338.84	6.47
C59	N	C	–		H	NO_2	H	H	1025.71	5.99
C60	N	C	–	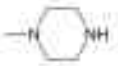	H	NO_2	H	H	1715.16	5.77
C61	N	C	–	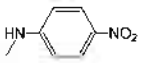	H	NO_2	H	H	585.59	6.23
C62	N	C	–	OCH_3	H	Cl	H	H	357.4 ± 87.61	6.45
C63	N	C	–	OC_2H_5	H	Cl	H	H	585.06 = 65.06	6.23
C64	N	C	–	OC_3H_7	H	Cl	H	H	438.00 = 53.46	6.36
C65	N	C	–	OC_4H_9	H	Cl	H	H	467.23 + 139.69	6.33
C66	N	C	–	OC_2H_5	H	CF_3	H	H	496.73 = 97.87	6.30
C67	N	C	–	OC_3H_7	H	CF_3	H	H	399.48 = 16.37	6.40
C68	C	C	H	H	H	NO_2	H	H	164.30 ± 4.22	6.78
C69	C	C	H	H	H	NO_2	H	H	8.43 ± 0.45	8.07
C70	C	C	H	H	H	NO_2	H	H	1.90 ± 0.15	8.72

Table 2. Summary of the PLS Runs with 8 CoMFA Sets

	I[a]		II[b]		III[c]		IV[d]	
Grid Spacing	2 Å	1 Å	2Å	1 Å	2 Å	1 Å	2 Å	1 Å
ONC[e]	7	9	6	8	7	8	7	9
q^{2f}	0.531	0.604	0.614	0.744	0.552	0.645	0.510	0.577
r^{2g}	0.924	0.964	0.907	0.966	0.914	0.957	0.890	0.960
SEE[h]	0.353	0.248	0.387	0.237	0.378	0.269	0.426	0.259
F[i]	107.685	176.511	102.549	218.096	93.656	168.160	71.719	161.902
SF[j]	83.7	87.0	78.8	83.8	80.2	85.2	80.4	85.7
EF[k]	16.3	13.0	21.2	16.2	19.8	14.8	19.6	14.3

[a]No region focusing. [b]weight by StDev*Coefficient region focusing. [c]weight by Discriminant Power region focusing. [d]weight by Modeling Power region focusing. [e]Optimum number of component. [f]Cross-validated r^2. [g]Non-cross-validated r^2. [h]Standard error estimate. [i]Fraction of explained versus unexplained variance. [j]Contribution of steric field. [k]Contribution of electrostatic field.

CoMFA region focusing. CoMFA region focusing[16] is a method of application of weights to the lattice points in a CoMFA region to improve q^2 as reducing the random but cross-correlated "brown" noise in the data matrix going into the analysis (brown noise is one reason why q^2 often falls off at grid spacing much below 2 Å). To selectively re-weight the grid points in a region, a new CoMFA column using the focused region file is created and the model is re-driven. Here three values as weight, such as StDev*Coefficients, Discriminant Power, and Modeling Power, were applied to get the better model.

Partial least square (PLS) analysis. PLS method was used to linearly correlate the activities with the CoMFA values. To avoid over-fitted 3D QSAR, the optimum number of components (ONC) used in the model derivation is chosen from the analysis with the highest cross-validated correlation coefficient (q^2).

The cross-validated q^2 quantifies the predictive ability of the model. It was determined by a leave-one-out (LOO) procedure of cross-validation in which one compound is removed from the dataset and its activity is predicted using the model derived from the rest of the dataset. During the cross-validation test, the sum of the squared prediction error called the predictive residual sum of squares (PRESS) is calculated for the model with each PLS component. After the predictive quality of the best correlation model is determined, the ONC is employed to do no validation PLS analysis to get the final model parameters such as correlation coefficient (r^2), standard error of estimate (SEE) and F value. The quality of the final CoMFA model is measured by two statistical parameters: r^2 and q^2. The value of q^2, which indicates the predictive capacity of the model, should be greater than 0.40 (in this calculation, q^2 is greater than 0.5); and the value of r^2, which shows the self-consistency of the model, should be greater than 0.90.

Results and Discussion

The results of QSAR analyses for 8 sets were summarized in Table 2.

From this table, we could find that the results were sensitive to the grid interval, *i.e.*, the models having grid size

Table 3. Predicted activities (PA) versus experimental activities (EA, pK_i) and their residuals

No.	EA	PA	Residual	No.	EA	PA	Residual
C1	9.77	9.49	0.28	**C36**	8.25	8.57	0.32
C2	8.07	8.54	0.47	**C37**	8.40	8.67	0.27
C3	9.44	9.16	0.28	**C38**	6.49	6.39	0.10
C4	9.58	9.30	0.28	**C39**	5.86	5.95	0.09
C5	9.49	9.67	0.18	**C40**	6.16	6.29	0.13
C6	8.77	8.57	0.20	**C41**	6.48	6.29	0.19
C7	7.90	7.64	0.26	**C42**	8.49	8.23	0.26
C8	9.62	9.53	0.09	**C43**	8.23	8.41	0.18
C9	8.01	8.07	0.06	**C44**	8.65	8.45	0.20
C10	8.85	8.59	0.26	**C45**	6.31	6.36	0.05
C11	7.40	7.40	0.00	**C46**	7.45	7.72	0.27
C12	7.10	7.12	0.02	**C47**	7.30	6.98	0.32
C13	7.92	7.91	0.01	**C48**	6.34	6.50	0.16
C14	10.77	9.78	0.99	**C49**	6.52	6.67	0.15
C15	8.71	9.13	0.42	**C50**	6.64	6.46	0.18
C16	8.28	8.22	0.06	**C51**	6.99	6.99	0.00
C17	7.17	7.13	0.04	**C52**	6.05	5.80	0.25
C18	7.21	7.23	0.02	**C53**	5.46	5.44	0.02
C19	7.22	7.31	0.09	**C54**	6.99	6.87	0.12
C20	6.90	6.92	0.02	**C55**	6.54	6.78	0.24
C21	6.84	6.72	0.12	**C56**	6.54	6.83	0.29
C22	6.64	6.73	0.09	**C57**	6.66	6.77	0.11
C23	8.89	8.92	0.03	**C58**	6.47	6.56	0.09
C24	10.30	10.28	0.02	**C59**	5.99	6.05	0.06
C25	7.62	7.94	0.32	**C60**	5.77	5.91	0.14
C26	8.43	8.25	0.18	**C61**	6.23	5.99	0.24
C27	7.69	7.70	0.01	**C62**	6.45	6.48	0.03
C28	7.13	6.94	0.19	**C63**	6.23	6.36	0.13
C29	8.48	8.97	0.49	**C64**	6.36	6.06	0.30
C30	8.77	8.94	0.17	**C65**	6.33	6.47	0.14
C31	9.04	9.16	0.12	**C66**	6.30	6.07	0.23
C32	8.24	8.27	0.03	**C67**	6.40	6.26	0.14
C33	6.94	6.98	0.04	**C68**	6.78	6.76	0.02
C34	6.50	6.55	0.05	**C69**	8.07	8.22	0.15
C35	8.57	8.60	0.03	**C70**	8.72	8.61	0.11
PRESS[a]							3.53

[a]PRESS = Σ (EA−PA)^2

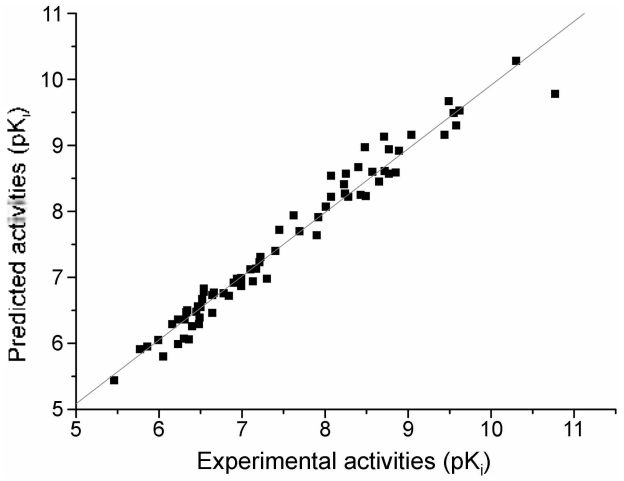

Figure 2. Predicted versus experimental activities of compounds in the training set. (r = 0.983).

of 1 Å showed higher r^2_{cv} values than those for the 2 Å grid (default value) and the model applying StDev*Coefficient region focusing gave a better result.

Comparison of CoMFA maps obtained using different grid spacing demonstrates that 1 Å grid model can describe fields available to each atom more closely and thus more accurately and dense map can be obtained even though it requires excess computer time.

Among the 8 models tested, the best predictive model was the fourth model having higher cross-validated and non-cross-validated correlation (r^2_{cv} = 0.744, r^2_{ncv} = 0.966) and proper ONC value. This model gives an ONC value of 8 and the relative contribution of steric and electrostatic potential to the CoMFA map was found to be 83.8 and 16.2%, respectively. This model showed strong dependence on the steric effect.

The biological activities of the antagonists in training set were compared with the corresponding predicted values (Table 3 and Figure 2). The residual value for each of the 70 antagonists and the PRESS were shown together. The predictive power of CoMFA for Model 4 is evident from Table 3 and Figure 2 which show good linear correlation (slope = 0.97, intercept = 0.26, regression = 0.983, n = 70) and small difference between predicted and actual values.

This result shows that our CoMFA analysis is good for correlating physicochemical properties with biological activity and theoretical activity from CoMFA can predict experimental value accurately.

The best way to evaluate the predictability of a CoMFA model is to predict theoretical pK$_i$ values for some compounds whose experimental values are known but not included in the training set (called test set). Eleven molecules (T1~T11) chosen for testing were shown in Table 4. Each of these structures was built up by starting from the template molecule in the set and performing necessary structural changes. New structures were also minimized using the same method applied to the compounds in the training set.

The PRESS, which is defined as the sum of squares of the differences between predicted and the observed values of the activity, is 4.07 (Table 5). Although this PRESS is larger than that of training set, this is enough to verify the power of CoMFA model.

The equations produced from a PLS analysis can contain large numbers of coefficients, so the usual way to visualize CoMFA results is through contour map of the PLS coefficients. These maps show regions where differences in molecular fields are associated with differences in biological activity. The contour plots give a direct visual indication as to which parts of the molecules differentiate activities of the compounds in the set under study.

Figures 3 and 4 show the CoMFA steric and electrostatic contour maps deduced from 70 compounds using the best

Table 4. Test set compounds and their biological activities

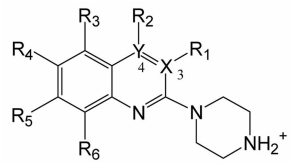

No	X	Y	R_1	R_2	R_3	R_4	R_5	R_6	K_i (nM)	pK_i
T1	C	C	C_3H_6Cl	H	H	NO_2	H	H	1.08 ± 0.17	8.97
T2	C	C	C_4H_9	H	H	NO_2	H	H	0.55 ± 0.09	9.26
T3	C	C	C_6H_5	H	H	NO_2	H	H	20.61 ± 2.08	7.69
T4	C	C	H	H	C_3H_7	NO_2	H	H	23.92 ± 0.30	7.62
T5	C	C	H	H	H	CN	H	H	7.49 ± 2.32	8.13
T6	C	C	C_4H_9	Cl	H	NO_2	H	H	42.88 ± 6.31	7.37
T7	C	N	CH_3	–	H	NO_2	H	H	61.70 ± 1.29	7.21
T8	N	C	–	OCH_3	H	NO_2	H	H	33.65	7.47
T9	N	C	–	OC_2H_4F	H	NO_2	H	H	95	7.02
T10	N	C	–	OC_4H_9	H	NO_2	H	H	610.53 ± 93.77	6.20
T11	N	C	–	OCH_3	H	CF_3	H	H	953.90 ± 993.13	6.02

Table 5. Experimental and predicted activities of 11 compounds and their residuals in the test set

No.	EA	PA	Residual
T1	8.97	9.58	0.61
T2	9.26	8.51	0.75
T3	7.69	8.53	0.84
T4	7.62	8.24	0.62
T5	8.13	8.77	0.64
T6	7.37	7.96	0.59
T7	7.21	7.93	0.72
T8	7.47	7.13	0.34
T9	7.02	6.64	0.38
T10	6.20	6.87	0.67
T11	6.02	6.27	0.25
PRESS[a]			4.07

[a]PRESS = Σ (EA−PA)^2

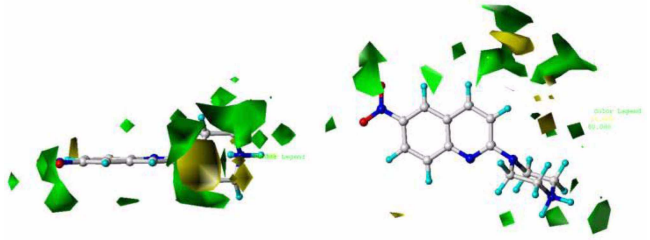

Front view Top view

Figure 3. Steric contour plot of the best CoMFA model.

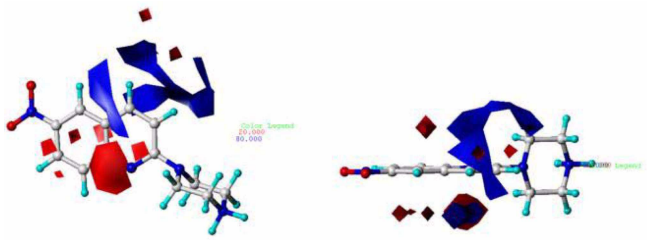

Front view Top view

Figure 4. Electrostatic contour plot of the best CoMFA model.

Model 4 (Table 2) respectively. The contours of the steric map are shown in yellow and green, and those of the electrostatic map are shown in red and blue. Greater values of bioactivity measurement are correlated with bulkier near green and less bulky near yellow and more positive charge near blue and more negative charge near red.

Here, contouring levels are at the default values of 80% and 20%. To show the spatial relationship of the contours more clearly, 6-NQ (C1) is displayed.

The steric contour plot shows three well-defined regions. The first is a green one close to the C_4 position and the second is green region spread to the outside of C_3, and the last is yellow one close to C_3-C_4. That is, main steric positive and negative potential fields are located near the surrounding of C_3-C_4 position.

Even though the electrostatic contribution in CoMFA analysis is low, Figure 4 indicates that above mentioned region is also important electrostatically. Up and down region of C_3~C_5 in aromatic ring is favorable for positive charge. While, surrounding region of N_1 is disfavorable. While quipazine itself has lower affinity (pK_i = 7.20), 6-nitroquipazine has high binding affinity (pK_i = 9.77).

In order to systematically analyze the bioactivity of the SERT antagonists, substituents on the quipazine ring are reclassified as R_1~R_6. Activities of compounds in the training set are tabulated along with their substituent type (Table 1). Entire compounds can be divided into several groups based on their structural features. Several important relationships between structure and bioactivity are found.

First of all, a nitro group at the C_6 position plays a pivotal role in retaining strong binding affinity for SERT. That is, 6-nitroquipazine is 10 times more potent than **C30~C31** having halogen atom on R_4 position.

Secondly, bulkier group at R_1 doesn't lower bioactivity. For example, **C4** and **C5** has similar pK, values (9.59 and 9.49, respectively) with 6-nitroquipazine (9.77). But, when more expanded substituents were located at R_1, it was found that introduction of pentyl or isopropyl (**C6** or **C38**) or phenyl (**C39~C41**) group at R_1 position shows decrease in bioactivity. Therefore, slightly bigger group is required in this position for more favorable interaction.

Thirdly, **C16~C22** compounds having a ring or heavy substituent at R_2 show decrease in binding affinity. In the diverse substitutions at R_2 position, **C14** (substituted with Cl) shows highest activity, and the case of having Br has also high activity. Cl on the R_2 position gave conspicuous improvement, but additional introduction on the other position didn't show good result anymore.

Also, substitution of ethylene group at R_3 improved the activity (**C24**). Additional introduction of a nitro group at C_7, C_8 positions or direct ring connection and substitution of carbon (C_3 or C_4 position) by nitrogen didn't give any meaningful result.

Conclusion

3D-QSAR studies of quipazine analogues acting as the SERT inhibitor were performed with CoMFA method. Total 8 models were constructed and the best model, using close 1 Å grid spacing and StDev*Coefficients weight value gave better correlation result. The obtained CoMFA model provided significant correlation and predictive ability statistically and could be potentially helpful in the design of novel and more potent SERT inhibitors.

Acknowledgement. This work was supported by INHA UNIVERSITY Research Grant.

References

1. Lucki, I. *Biol. Psychiatry* **1998**, *44*, 151.
2. Frazer, A. J. *Clin. Psychiatry* **1997**, *6*, 9.
3. Rudnick, G.; Clark, J. *Biochim. Biophys. Acta* **1993**, *1144*, 249.

4. Clark, J. A. *J. Biol. Chem.* **1997**, *272*, 14695.
5. Pacholczyk, T.; Blakely, R.; Amara, S. *Nature* **1991**, *350*, 350.
6. Blakely, R.; Berson, H.; Fremeau, R.; Caron, M.; Peek, M.; Prince, H.; Bradely, C. *Nature* **1991**, *354*, 66.
7. Hashimoto, K.; Goromaru, T. *Eur. J. Pharmacol.* **1990**, *180*, 272.
8. Hashimoto, K.; Goromaru, T. *Neuropharmacology* **1991**, *30*, 113.
9. Hashimoto, K.; Goromaru, T. *Fundam. Clin. Pharmacol.* **1990**, *4*, 635.
10. Hashimoto, K.; Goromaru, T. *Pharmacol. Exper. Ther.* **1990**, *225*, 146.
11. Cramer, R. D.; Patterson, D. E.; Bunce, J. D. *J. Am. Chem. Soc.* **1988**, *110*, 5959.
12. Lee, B. S.; Chu, S.; Lee, B. C.; Chi, D. Y.; Choe, Y. S.; Jeong, K. J.; Jin, C. *Bioorg. Med. Chem. Lett.* **2000**, *10*, 1559.
13. Lee, B. S.; Chu, S.; Lee, B.-S.; Chi, D. Y.; Choe, Y. S.; Jin, C. *Bioorg. Med. Chem. Lett.* **2002**, *12*, 811.
14. Lee, B. S.; Chu, S.; Lee, B. C.; Lee, B.-S.; Chi, D. Y.; Choe, Y. S.; Kim, S. E.; Song, Y. S.; Jin, C. *Bioorg. Med. Chem.* **2003**, *11*, 4949.
15. *SYBYL*, version 6.8; Tripos Inc.; 1669, St. Louis, Missouri, USA.
16. Lindgren, F.; Geladi, P.; Rännar, S.; Wold, S. *J. Chemometrics* **1994**, *8*, 349.